

1 Proposed allosteric inhibitors bind to the ATP site of CK2 α

2

3 Paul Brear^{1*}, Darby Ball², Katherine Stott¹, Sheena D'Arcy² and Marko Hyvönen^{1*}

4 ¹Department of Biochemistry, University of Cambridge, UK

5 ²Department of Chemistry and Biochemistry, The University of Texas at Dallas, USA

6 *Correspondence to Paul Brear (pdb47@cam.ac.uk) and Marko Hyvönen (mh256@cam.ac.uk)

7 **Keywords:** CK2 α , inhibitor, ATP-competitive, kinase, biophysics

8 **Abstract**

9 CK2 α is a ubiquitous, well-studied protein kinase that is a target for small molecule inhibition, for
10 treatment of cancers. While many different classes of ATP-competitive inhibitors have been
11 described for CK2 α , they tend to suffer from significant off-target activity and new approaches are
12 needed. A series of inhibitors of CK2 α has recently been described as allosteric, acting at a previously
13 unidentified binding site. Given the similarity of these inhibitors to known ATP-competitive
14 inhibitors, we have investigated these further. In our thorough structural and biophysical analyses,
15 we have found no evidence that these inhibitors bind to the proposed allosteric site. Rather, we
16 report crystal structures, competitive ITC and NMR, HDX mass spectrometry and chemoinformatic
17 analyses that all point to these compounds binding in the ATP pocket. Our crystal structures
18 however do show that the proposed allosteric site can bind ligands, just not those in the previously
19 described series. Comparison of our results and experimental details with the data presented in the
20 original report suggest several reasons for the disparity in our conclusions, the primary reason being
21 non-specific inhibition by aggregation.

22 **Introduction**

23 Potent inhibitors of kinases have existed for some time and the majority of these bind in the active
24 site of the kinase, competing with the co-factor ATP^{1,2}. Because of the significant conservation of the
25 ATP binding site, kinase inhibitors often suffer from poor selectivity^{3–7}. This poor selectivity is a
26 disadvantage for several reasons. Firstly, promiscuous inhibitors tend to manifest off-target toxicity if
27 used therapeutically and, to combat this, end up being used at suboptimal concentrations^{8,9}. Secondly,
28 they are poor chemical tools as they cannot provide unambiguous answers to target validation
29 questions. In order to develop more selective inhibitors of kinases, a promising strategy is to target
30 sites outside the highly conserved ATP pockets. This leads to increased selectivity as these sites are
31 structurally not constrained by the shared property of binding to ATP and therefore tend to be less
32 conserved among different kinases^{10–13}. When developing inhibitors that bind outside the primary ATP
33 site, it is vital that the new sites are thoroughly validated biochemically, biophysically, and structurally

34 to confirm the inhibitor binding mode unambiguously. Often inhibitors are identified as being
35 allosteric if they are shown to be non-competitive in biochemical assays. However, this data can be
36 misinterpreted, as non-specific inhibitors also often show similar non-competitive behaviour¹⁴. This
37 problem can be further compounded by moderate/weak affinity of the hits being investigated, as they
38 must be used at higher concentrations, which makes secondary binding more likely. Therefore,
39 apparent allosteric behaviour must be very carefully validated to ensure that vital time and resources
40 are not wasted on optimising these inhibitors further.

41 CK2 α has a long history as a target for drug discovery, due to its ubiquitous role in multiple diseases
42 such as cancer and fibrosis^{15–17}. CK2 α is an unusual kinase in that it is constitutively active and does
43 not require phosphorylation for activation¹⁸. It is also a highly promiscuous kinase with hundreds of
44 recorded cellular substrates.¹⁹ Inhibition of CK2 α has been achieved mostly through an ATP-
45 competitive mechanism and a number of high affinity inhibitors of distinctly different chemotypes
46 are known and characterized structurally^{17,20–27}. Despite significant effort, most inhibitors have poor
47 selectivity, although claims are often made to the contrary^{28–32}. For example, the clinical trial
48 candidate CX-4945 inhibits at least ten other kinases with nanomolar affinity (see Table S1 in Brear
49 et al.²⁵).

50 We have recently demonstrated a new approach to CK2 α inhibition. By using a cryptic so-called α D
51 pocket just below the active site as an anchoring point, we have been able to develop highly
52 selective inhibitors of CK2 α ²⁵. The most potent of these is the most specific CK2 α inhibitor reported
53 to date, CAM4066²⁵. The fragment-based development of these inhibitors was supported by a
54 significant amount of structural data to identify the optimal α D site anchor moiety and subsequent
55 growth of the fragment to the ATP site²⁷. In addition to active site targeting, another approach is the
56 inhibition of CK2 α binding to its scaffolding partner CK2 β . This method has the potential to generate
57 specific inhibitors that affect only a subset of CK2 substrates^{24,33} and has led to some initial
58 encouraging success that requires further development^{24,33,34}.

59 Recently, a series of CK2 α inhibitors (Series A, SI Fig. 1), proposed to bind in a novel site (Site A, SI
60 Fig. 2) just outside of the highly conserved ATP site, has been published^{35,36}. The authors used
61 enzymatic assays, native mass spectrometry and competitive ligand-based NMR studies to
62 characterize the mode of inhibition. They interpret their data as supporting an allosteric mechanism.
63 While their data were presented as supporting non-ATP-competitive inhibition, there were several
64 reasons why we speculated that the mechanism of inhibition by these molecules was not necessarily
65 allosteric. In particular: the enzyme assays showed mixed mode inhibition; ATP analogues were
66 replaced in NMR studies; high affinity ligands showed unexpected signal in ligand-based NMR

67 experiments; and, mutations close to the ATP site affected inhibitory potential^{35,36}. Our motivation
68 to investigate these inhibitors in more detail arose from the somewhat conflicting data presented,
69^{35,36} as well as the chemical properties of these new inhibitors, which are not unlike known ATP
70 competitive kinase inhibitors.

71 We have used several orthogonal biophysical and structural methods for the characterization of the
72 binding mode of these new CK2 α inhibitors and we find no evidence for interaction with the
73 proposed allosteric site (Site A). We show, using crystal structures, competitive ITC and NMR,
74 hydrogen-deuterium exchange mass spectrometry (HDX) and computational analyses of the ligand
75 structures, that these molecules are clearly binding to the ATP site of the kinase. It thus seems likely
76 that most of the inhibitory effect, if not all, comes from traditional type I inhibition of the kinase
77 through orthosteric competition with ATP.

78 Results

79 Chemoinformatic analysis

80 The structures of the compounds presented in the original papers and their comparison to other
81 validated kinase and CK2 α inhibitors raised concerns over the claim that these compounds had a
82 novel binding mode. The conserved scaffold of the compounds shares significant similarity to many
83 established and well validated kinase inhibitors that bind in the ATP site (Fig. 1)^{27,37-63}. This scaffold
84 consists of a central thiazole ring that is connected directly to a phenyl group on one side and to a
85 benzoic acid moiety through an amine on the other side (Fig. 1A). We have used two representative
86 compounds from Series A for further investigation, which we denote **1** and **2** (these were referred to
87 as **6** and **27** respectively in the original papers^{35,36}). **1** was chosen as much of the validation of Series
88 A and Site A relied upon this compound³⁵. **2** was chosen as it was the highest affinity inhibitor
89 reported in Series A.³⁶ A search of the Protein Data Bank (PDB, <http://www.pdb.org>) for ligands that
90 bind to serine/threonine kinases (EC=2.7.11.1) and contain a benzoic acid group, which is a critical
91 part of the inhibitors in question (Fig. 1B), identified 49 molecules. Of these, 46 bind in the ATP site
92 and the remaining three bind in interface sites that do not exist in CK2 α (SI Table 1). Narrowing the
93 search by inclusion of the amine that links the benzoic acid to the thiazole ring identified 15 ligands
94 (SI Table 2). Of these ligands, all 15 bind in the ATP site. When a similar search was performed on
95 CK2 α , 14 ligands were identified, all of which bound in the ATP site (SI Table 3). Four representative
96 structures of these compounds are shown in Fig. 1C. All of these inhibitors display the same binding
97 mode where the binding to CK2 α is dominated by the interaction between the carboxylic acid and
98 the ζ -amino group of Lys68 (Fig. 1C). Further refining the search to include only compounds that also
99 bind in the hinge region, similar in structure to the thiazole-amine group of **1**, identified eight
100 inhibitors (SI Table 4). These compounds, including **CX4945**, an extensively validated ATP-

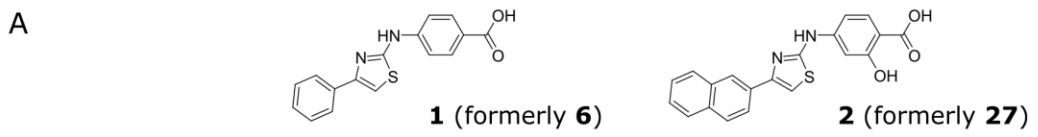
101 competitive CK2 α inhibitor currently in clinical trials, interact with the hinge and Lys68⁴⁷. Overlaying
102 the 2D structure of **1** with **CX4945** shows that **1** could replicate the binding mode of **CX4945** (SI Fig 2)
103 and bind in the ATP site with its carboxylic acid interacting with Lys68 and amine hydrogen bonding
104 with the hinge (Fig 1C). Indeed, modelling of **1** into the ATP site of CK2 α replicates the
105 crystallographic binding mode of **CX4945** (SI Fig 2). The carboxylic acid is interacting with Lys68 and
106 an ATP site water as predicted and the hydrophobic core of the molecule is sandwiched between
107 Met163 and Val66. The amine is not predicted to interact with the hinge. However, the benzyl group
108 is predicted to bind in a similar position to the benzyl chloride of **CX4945**.

109 Further evidence in support of our hypothesis that **1** may bind in the ATP site comes from the
110 analysis of a fragment-based X-ray crystallographic screen against CK2 α ²⁷ previously performed at
111 our lab. One purpose of fragment-based X-ray crystallographic screening is to use the fragments to
112 probe the target protein and identify binding hotspots⁶⁴. From the screen of 354 fragments, 21 were
113 identified as binding to CK2 α . All 21 bound in the ATP site and interacted with Lys68²⁷. 19 of the
114 CK2 α -binding fragments were structurally related to **1** and contained a carboxylic acid moiety that
115 mediated this interaction (SI Fig. 3). The preference of CK2 α for binding ligands with a carboxylic acid
116 in this position is further supported by the serendipitous binding of acetate. Acetate ions can be
117 utilised as a very low molecular weight probe to identify binding sites for carboxylic acids⁶⁴. In CK2 α
118 structures deposited to the PDB, at least nine binding sites for acetate can be identified (SI Fig. 4).
119 Among these sites are the Lys68 hotspot in the ATP site, the CK2 β interface and the substrate-
120 binding pocket. Notably, none of the nine sites overlaps with Site A, the proposed binding site of **1**.
121 When such a conserved binding mode is observed for an ATP site-binding pharmacophore, it seems
122 unlikely that inhibitors with significant structural similarity would not also bind to the ATP site. These
123 observations led us to initiate additional studies to investigate the binding mode of these inhibitors
124 using two compounds (**1** and **2**, Fig. 1A) from the original publications.

125

126

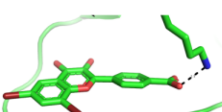
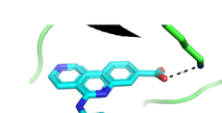
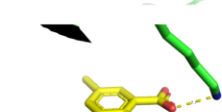
127



B

Compound 1	PDB search terms		Number of ligand hits	
	Ligand search	Text search	ATP site	non-ATP site
		+ "2.7.11.1"	= 46	3
		+ "2.7.11.1"	= 15	0
		+ "Casein kinase II"	= 14	0
		+ "Casein kinase II"	= 8	0

C

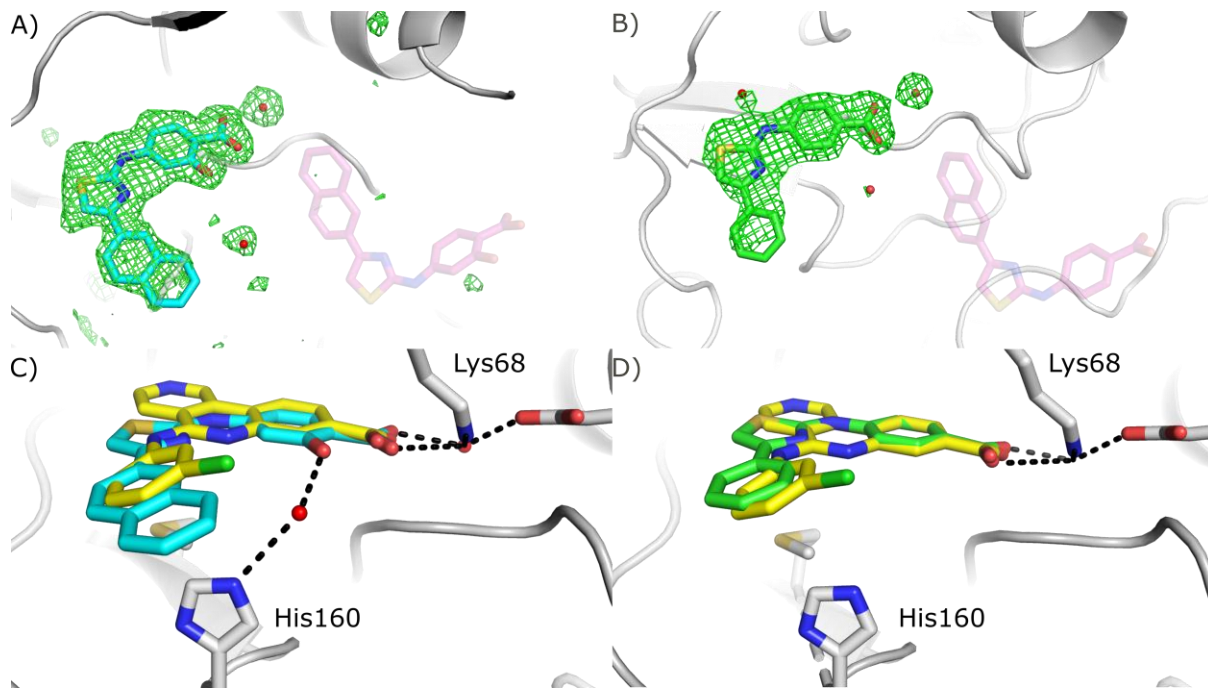
Compound 1	CK2 α Ligand		Binding Site	PDB code	Binding mode
	Hinge region	Lys binding			
			ATP site	4UB7	
		CX4945	ATP site	3NGA	
			ATP site	3AXW	
			ATP site	5CSP	

128

129 **Figure 1. Conserved pharmacophore binding in the ATP site of protein kinases** (A) The structures of **1** and **2**,
130 denoted **6** and **27** respectively in the original studies. (B) A summary of the analysis of the established ligands
131 that bind to Ser/Thr protein kinases (EC number 2.7.11.1) or CK2 α in the ATP site. (C) The structures of the
132 four CK2 α inhibitors and their protein-bound crystal structures which contain a benzoic acid group that binds
133 in the ATP site^{27,37,46–55,38,56–63,39–45}.

134 X-ray crystallographic analysis
135 The original publication contained no structural data on the inhibitor binding mode. In fact, the
136 authors state that 'cocrystallisation attempts aimed at elucidating the non-ATP competitive binding
137 mode of 2-aminothiazole derivatives with CK2 α were not successful'^{35,36}. We have rectified this and
138 have determined structures of both **1** and **2** in complex with CK2 α (Fig. 2, SI Table 5). These
139 structures were obtained by soaking the compounds into CK2 α crystals at 10 mM for 16 hours. The
140 crystals diffracted at less than 2 Å resolution and unambiguous positive difference electron density
141 corresponding to both **1** and **2** can be clearly seen in the ATP site before the ligands were included
142 (Fig. 2A and 2B, SI Fig. 5). As we predicted, the carboxylic acid groups of both compounds interact
143 directly with Lys68 like the carboxylic acid of **CX4945** (Fig. 2C and 2D). The remainder of the
144 molecules however, each have their own binding nuances. The amine of the benzylamine of **1**
145 interacts very weakly with the hinge region backbone nitrogen of Val116 via a bridging water
146 molecule whereas the OH group of **2** interacts with His160, via a bridging water, which pulls the
147 amine of the benzylamine further away from the hinge region and prevents interactions with the
148 hinge (Fig. 2C and 2D). The 5-membered rings from **1** and **2** stack on top of Met163 which leads to
149 the naphthyl ring of **2** stacking on top of His160 at the entrance to the ATP site. The observed
150 binding mode agrees well with the binding mode of established ATP site inhibitors of CK2 α , such as
151 **CX4945**. No density corresponding to either **1** or **2** was observed in the proposed allosteric binding
152 site (Site A, SI Fig. 5), despite the high concentration of the ligand (>1,000-fold excess over K_D) used
153 for soaking. The binding mode of **1** in the ATP site of CK2 α observed in the crystal structure agrees
154 well with that predicted by the modelling study (SI Fig. XXXX).

155
156
157
158

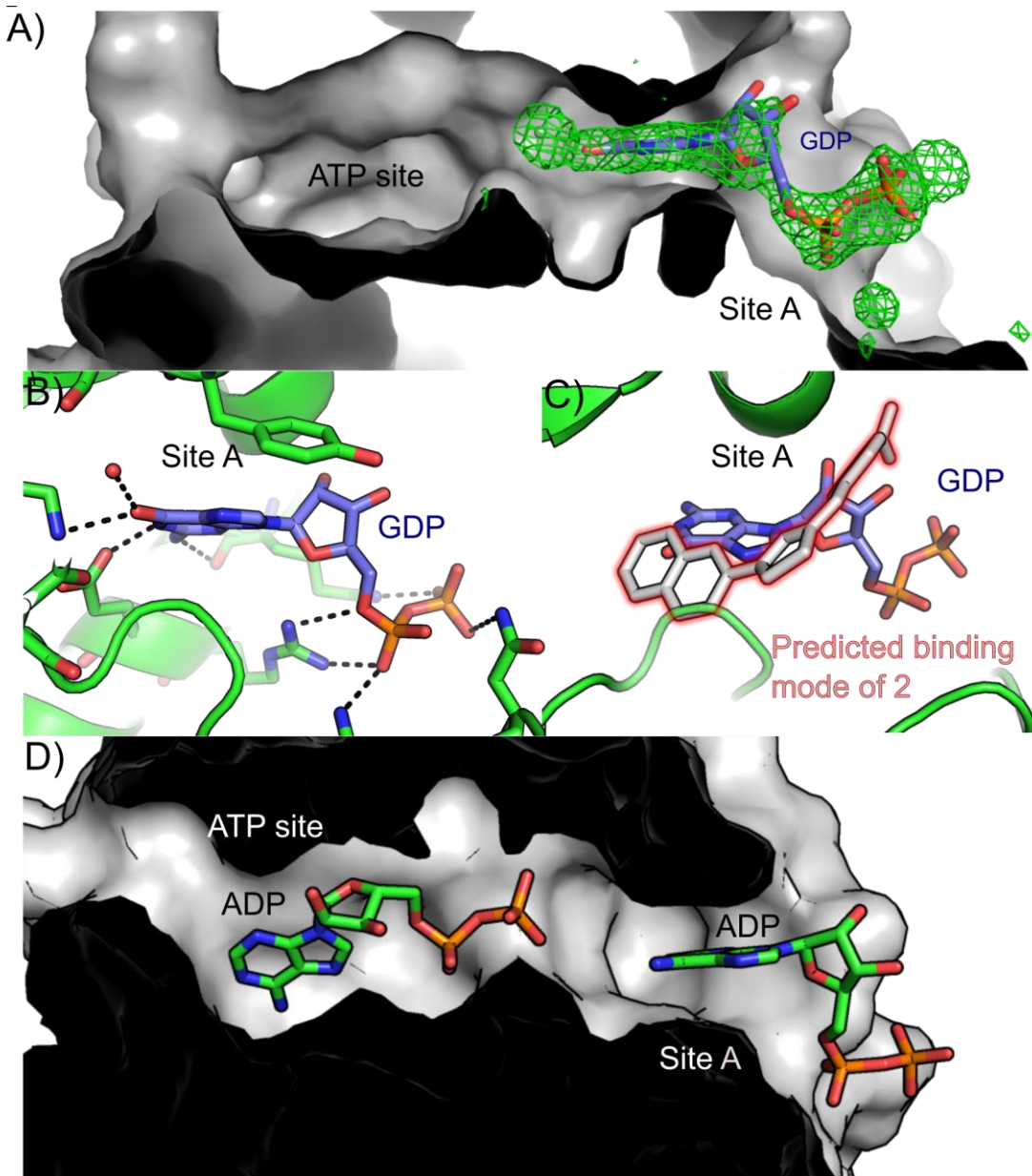


159
160 **Figure 2. Crystal structures of compounds 1 and 2 bound to CK2 α** (A) The Fo-Fc map (green, displayed at 3σ) in the ATP site and Site A before the ligand has been placed. Refined structure of **1** (green) has been superimposed on the ATP site (PDB: 6YPJ) and the predicted binding mode of **2** (transparent purple) is shown on Site A. (B) The Fo-Fc map (green, contoured at 3σ) for the ATP site and Site A before the ligand has been placed. Refined structure of **2** (blue) has been superimposed on the ATP site (PDB: 6YPG) and the predicted binding mode of **2** (transparent purple, from supplementary material of reference 34) is shown on Site A. (C) **1** (green) bound to CK2 α , (PDB: 6YPJ) with key interacting residues and H-bonding highlighted. (D) **2** bound to CK2 α (PDB: 6YPG), with key interacting residues and H-bonding highlighted. The structure of CX4945 (PDB: 3PE1, yellow) has been superimposed on the structure of **1** and **2** in panels C and D. Electron densities of the final, refined structures are shown in SI Fig. 6.

171
172 To reduce the impact that different crystal forms and packing may have on the accessibility of
173 binding sites and bias in the resulting complex structure, we have soaked the inhibitors into two
174 different crystal forms of CK2 α . One is obtained using an engineered form of CK2 α (referred to as
175 CK2 α KKK/AAA) in which lysines 74-76 are mutated to alanines to facilitate crystallization. These
176 lysines are in the vicinity of Site A and could affect binding of ligands to this site. However, these
177 lysines do not affect the ATP site and we show later that both **1** and **2** bind to CK2 α KKK/AAA and to
178 wild type CK2 α with the same affinity (see ITC measurements). The second crystal form (CK2 α SF)
179 has no mutations in the lysine-rich loop but has a substrate peptide fused to the N-terminus of the
180 protein, aimed at facilitating crystallization. In both crystal forms, we observe electron density for **1**
181 and **2** only in the ATP site, and not in the proposed allosteric site (Site A, SI Fig. 5).

182 The two crystal forms of CK2 α have been extensively used for the determination of CK2 α :ligand
183 complexes (66 structures currently in the PDB). More than eight different ligand binding sites can be

184 accessed by soaking into these crystal forms (SI Fig. 7), including the proposed allosteric site for **1**
185 and **2**, Site A. We have observed both ADP and GDP bound to Site A in crystal structures of wild type
186 CK2 α (PDB:6YPN) and in the KKK/AAA mutant (PDB:6YPK) (Fig. 3). The adenine and guanosine
187 rings sit in the hydrophobic pocket identified in the previous modelling work³⁵ and the diphosphate
188 interacts with Arg80 that has been identified as an acetate-binding hotspot (SI Fig. 4). This confirms
189 that Site A is accessible to ligands in these crystal forms and soaking with **1** or **2** would be expected
190 to result in clear electron density in the site, should they bind there. Indeed, ADP can be seen
191 simultaneously in both the ATP site and in Site A (Fig. 3D, PDB: 6YPN). These observations
192 demonstrate that binding in Site A does not in itself prevent binding in the ATP site and that if **1** or **2**
193 did bind in both sites, we would expect to see density corresponding to it. Furthermore, **1** and **2**
194 would be expected to bind predominantly in the highest affinity site and this site would dominate
195 the inhibition. These crystal structures prompted us to perform further experiments to
196 unambiguously establish the binding site in solution and verify the likely mode of inhibition for these
197 compounds.



198

199 **Figure 3.** Crystal structures of ADP and GDP binding to CK2 α Site A. (A) GDP binding in Site A. The Fo-
200 Fc map (contoured at 3 σ) centered on the proposed allosteric site. No density was observed in the
201 ATP site for GDP therefore the density in the ATP site was not shown for clarity. The CK2 α KKK/AAA
202 construct was used for this structure (PDB: 6YPK). B) The structure of GDP bound to CK2 α , with the
203 extensive H-bonding network shown by dotted lines (PDB: 6YPK). C) The proposed binding mode of 1
204 (PDB: 6YPJ) superimposed on the structure of GDP bound to CK2 α (6YPK). D) The structure of ADP
205 bound simultaneously in the ATP site and in Site A of WT CK2 α (PDB: 6YPN).

206 Hydrogen-deuterium exchange mass spectrometry
207 Hydrogen-deuterium exchange (HDX) allows the localization of interaction sites and conformational
208 changes in proteins. We have analysed the binding of four different classes of ligands to CK2 α (SI Fig.
209 8 and 9) using HDX. These ligands were: ADP and AMPPNP-Mg $^{2+}$, both of which bind across the

210 entire ATP site interacting with the hinge region and Lys68 (SI Fig. 8C and 8D);⁶⁰ **3**, which is a
211 fragment that binds only on the right hand side of the ATP site, interacting with Lys68⁶⁰ (SI Fig. 8E);
212 **4**, which is an α D site binder (SI Fig. 8G)²⁶ and **6** which links the α D site and the ATP site (SI Fig. 8F)²⁷.
213 We recovered 192 shared peptides from each of these HDX experiments that redundantly span
214 almost the entire sequence of CK2 α (SI Fig. 10). This allows for unbiased detection of ligand
215 interaction fingerprints across the whole of the protein. Binding can be identified by observing
216 changes in deuterium uptake between CK2 α alone and a concurrently run ligand-bound sample (SI
217 Table 6). We show all changes greater than ± 0.25 Da that have a p-value less than 0.01 in a Welch's
218 t-test (Fig. 4 and SI Fig. 11). Extended data for all peptides and timepoints are shown in the
219 Supplementary Information (SI Fig. 11 and a separate spreadsheet). For all the ligands, a decrease in
220 deuterium uptake is observed at late timepoints particularly for peptides containing residues 54-111
221 (sample peptides shown in SI Fig. 12). Since this change occurs with all the ligands, it appears to
222 result from general stabilization of the region termed the 'N-lobe', on ligand binding, rather than an
223 effect attributable to a specific site.

224 Addition of ADP and AMPPNP-Mg²⁺ causes clear changes in deuterium uptake in the ATP site (Fig. 4).
225 The largest change is a decrease in deuterium uptake for peptides covering residues 39-55 and 121-
226 131. Residues 39-55 correspond to the P-loop that interacts directly with the phosphates of ADP,
227 while residues 121-131 are the α D loop that does not interact directly with ADP or AMPPNP-Mg²⁺.
228 Protection occurs in the latter due to the interaction of the adenine ring with the hinge region that
229 directly links to and stabilizes the α D loop. These observations are similar to those previously
230 observed when binding of ATP analogues to other kinases has been studied^{65,66}. The observed
231 decreases in uptake are larger for AMPPNP-Mg²⁺ than ADP-Mg²⁺ because AMPPNP binds with a
232 higher affinity than ADP. To further probe interactions in a more localized area of the ATP site, we
233 used **3** that binds only at the right hand side of the ATP site (SI fig 8 E), coordinated to catalytic Lys68
234 (PDB: 5CSP)⁶⁰ (Fig. 4). With **3**, we see a decrease in deuterium uptake in the P-loop and no change in
235 the α D loop. The pattern of protection within the P-loop is also distinct, indicative of different
236 binding contacts being used by **3** compared to the ATP analogues. We can thus distinguish binding
237 in the entire ATP site, including interaction with the hinge, from binding on just one side where
238 Lys68 is located.

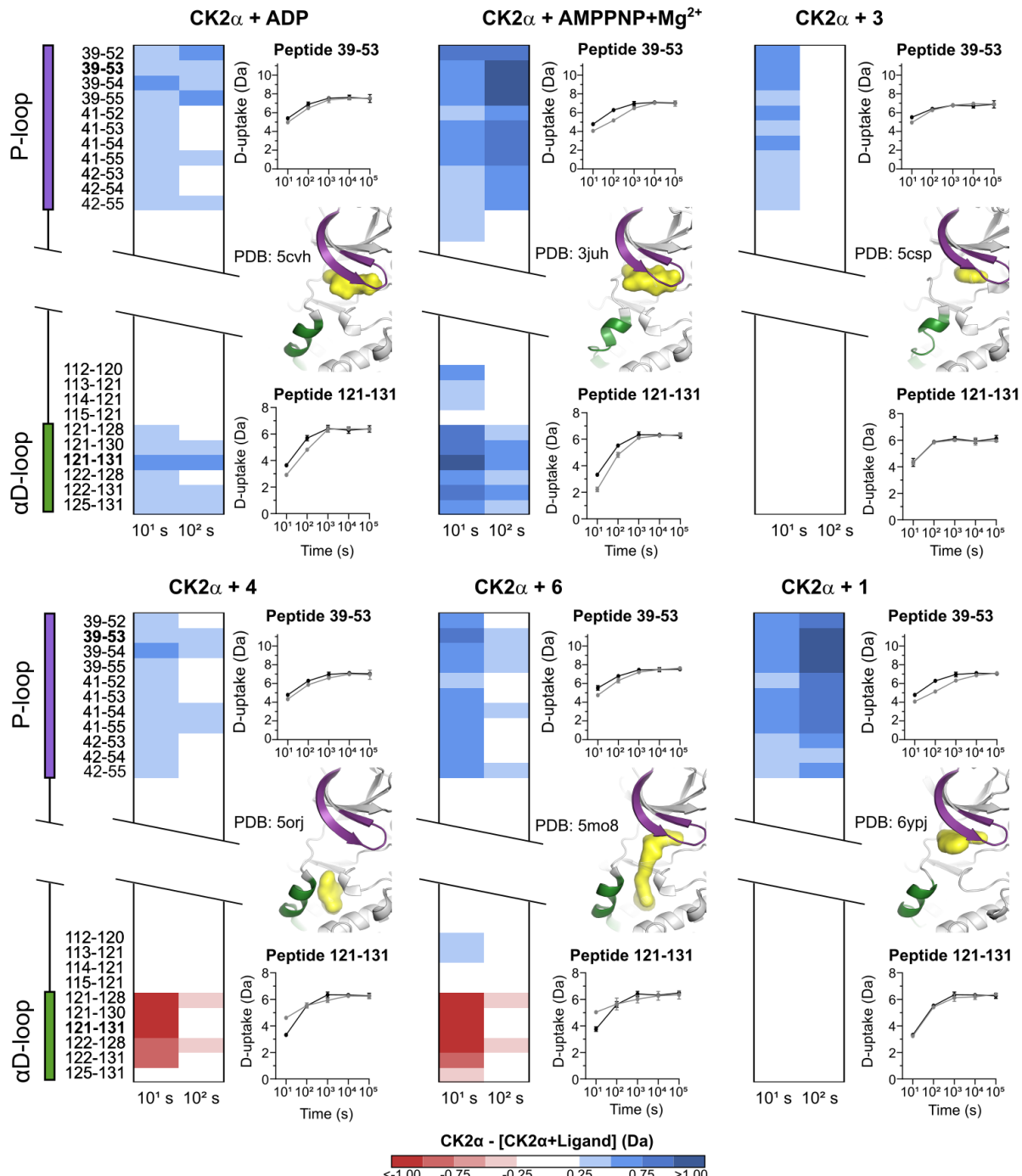
239 To ensure we could detect different binding sites with our HDX experiments, we used another well
240 characterized ligand (**4**) that binds to the α D pocket only (SI Fig. 8G)²⁶. This compound shows a
241 markedly different HDX fingerprint compared to the ATP analogues and **3** (Fig. 4). The largest
242 differences are seen in the α D loop, with binding of **4** resulting in increased uptake compared to
243 unbound CK2 α . Increased uptake in the α D loop is opposite to the decrease seen upon ADP and

244 AMPPNP-Mg²⁺ binding. This indicates that the binding of **4** in the α D pocket puts the loop in a more
245 flexible or open conformation amenable to exchange, as is seen in the crystal structure of CK2 α in
246 complex with **4** (PDB: 5ORJ). Finally, we characterised the HDX fingerprint for **6** that occupies both
247 the α D pocket and the ATP site. We observed a similar increase in uptake in the α D loop as with **4**
248 (Fig. 4). Compounds **4** and **6** also cause decreased uptake in the P-loop, with **6** showing more
249 protection than **4**, similar to the protection we observed with **3**.

250 All these fingerprints are consistent with the known binding modalities of these ligands to CK2 α and
251 can be used to identify the binding modes of new compounds. We performed the same experiments
252 to characterise the binding of compound **1** to CK2 α (Fig. 4). Addition of **1** to CK2 α causes decreased
253 uptake in the P-loop with a pattern and magnitude of change similar to the addition of AMPPNP-
254 Mg²⁺. However, no changes are observed in the α D pocket, as was observed with the addition of **3**.
255 These results are consistent with the binding mode seen in the crystal structures where **1** makes
256 significant hydrogen bonding just to Lys68 with only weak water-mediated interaction to the hinge
257 region. These data do not allow us to unequivocally eliminate binding at the proposed allosteric site.
258 However, if the allosteric binding mode were correct, two clear differences would be expected.
259 Firstly, a change in the uptake by residues 67-88, part of Site A, would be expected due to the main
260 interaction being with the acidic group of **1** (SI Fig. 8). We do not observe changes in uptake in this
261 region despite it being redundantly covered by eight peptides (SI Fig. 11). Secondly, no change in the
262 uptake by the P-loop would be expected since the modelling does not predict significant interactions
263 with that part of the protein. Interactions with the P-loop, such as that seen for **1**, are one of the
264 major features of ATP site binders, consistent with our structural characterization of **1** and
265 **CAM4066**.

266

267



268

269 **Figure 4.** HDX analysis of ligand binding to CK2 α . Heatmaps show the change in deuterium uptake
 270 upon binding of different ligands to apo CK2 α . Each panel, with the ligand listed on the top, shows
 271 the heatmaps for 10 s and 100 s time points for peptides corresponding to the P-loop and α D-loop,
 272 in comparison to unliganded CK2 α . All depicted changes are greater than ± 0.25 Da and have a p-
 273 value less than 0.01 in a Welch's t-test. The exact start and end residues for each peptide are shown
 274 on the left of the panels. Next to each heatmap are two graphs showing deuterium uptake for one
 275 peptide from each P-loop (top) and α D loop (bottom) for apo CK2 α (black) and CK2 α with ligand
 276 (grey). The Y-axis range is 80% of max D-uptake assuming the N-terminal residue undergoes 100%

277 back-exchange. Data have not been corrected for back-exchange. Error bars are $\pm 2\sigma$ derived from
278 three technical replicates. A structural diagram in between the uptake plots has the P-loop and α D
279 loop coloured purple and green, respectively, and the bound ligand in surface rendering in yellow.
280 Full HDX data are shown in SI Fig. 11 and available in the supplementary spreadsheet.

281 Ligand-observed NMR analyses
282 To further explore the binding of the new compounds to CK2 α , we have used various ligand-based
283 NMR methods, similar to the experiments in the original characterization of these molecules. We
284 were particularly concerned about the evidence for the simultaneous binding of **CX4945** and **1** due
285 to the presence of strong signals for **CX4945** in the STD NMR spectra. In order to observe a signal in
286 an STD spectrum, the saturation of protein resonances has to be transferred to the bound ligand,
287 which then dissociates to join the pool of bulk ligand in solution before it can be detected. This
288 means that the size of the signal for a given ligand is proportional to the amount of the ligand that
289 binds to *and* is released by the protein during the saturation step of the STD experiment. Therefore,
290 ligands with relatively fast association (k_{on}) and dissociation (k_{off}) rates give the largest signal.^{67,68}

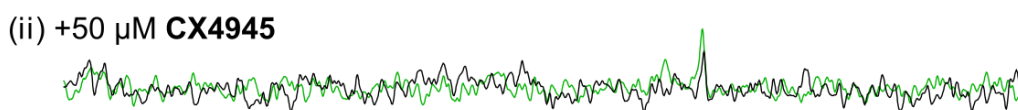
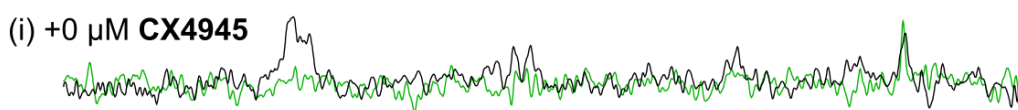
291 We have determined the off rate of **CX4945**, that binds to CK2 α with low nanomolar to picomolar
292 affinity⁴⁷, from CK2 α to be 0.0039 s^{-1} by SPR (SI Fig. 12). When ligands have k_{off} rates $<0.1\text{ s}^{-1}$, the
293 saturation cannot be transferred effectively to bulk ligand in solution resulting in no observable STD
294 effect⁶⁸. The experimentally determined off-rate for **CX4945** means that less than 1% of **CX4945**
295 would have dissociated after the 2-second saturation time used in the NMR pulse sequence. This
296 would mean that the concentration of saturated ligand in solution would be less than $0.1\text{ }\mu\text{M}$. This
297 difference would not be observable by NMR.

298 To resolve these issues, we have repeated the STD NMR studies reported in the original publication
299 ³⁵ and used two additional ligand-based NMR experiments, CPMG and Water-LOGSY⁶⁷, for further
300 validation. Our STD experiment shows that **1** binds to CK2 α , as revealed by detectable transferred ^1H
301 intensities (Fig. 5A(i)). However, when the same experiment is run in the presence of **CX4945**, a
302 significant reduction of the STD signals from **1** are observed, indicating direct competition between
303 the two ligands (Fig. 5A(ii)). In the original paper, strong **CX4945**-derived signals are also clearly
304 visible. The signals - which are comparable in magnitude to the much weaker binding ligand **1** - could
305 instead arise from non-specific binding of **CX4945** to lower affinity sites on CK2 α (as was shown by
306 native mass spectrometry³⁵), precipitation of **CX4945** leading to false positive signals in the
307 experiment or binding of CX4945 to soluble aggregates of **1**.

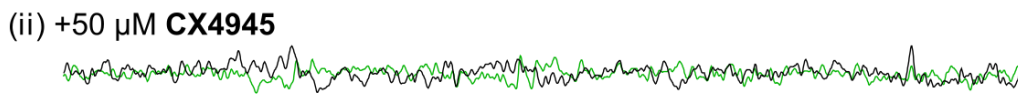
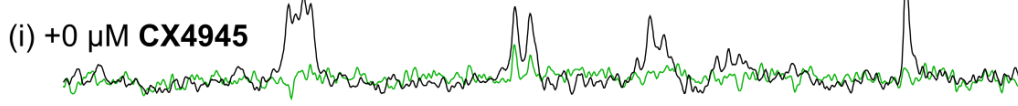
308 Given the disparity in the STD NMR experiments between our results and those in the original
309 report, we have also used CPMG and Water-LOGSY experiments. These exploit different NMR

310 phenomena (relaxation rates, transfer of saturation) to observe the binding of the ligand to the
311 protein⁶⁷. Using three different methods to observe the binding of the ligand reduces the chance of
312 experimental anomalies interfering with the outcome of the experiment. The Water-LOGSY
313 experiment shows clear binding of **1** to CK2 α and complete inhibition of binding in the presence of
314 **CX4945** (Fig. 5B). Similarly, in the CPMG experiment, an increase in the signal from the aromatic
315 protons of **1** was observed in the presence of **CX4945** indicating a reduction in binding of **1** to CK2 α
316 (Fig. 5C). In conclusion, all three ligand-observe NMR experiments show binding of **1** to CK2 α and in
317 all three experiments binding is abolished by **CX4945**, suggesting direct competition between these
318 two ligands as they bind to the same site.

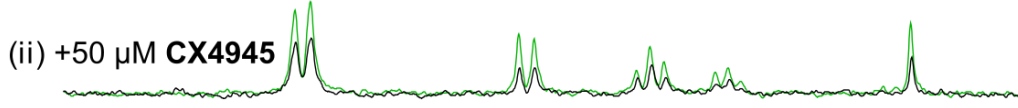
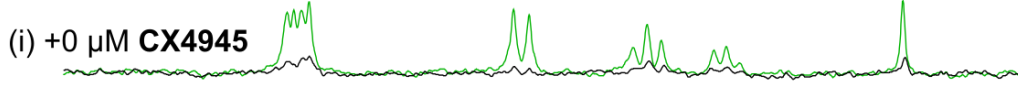
A



B



C



7.8 7.6 7.4 7.2 7.0 ppm

~~~~~ 0.5 mM **1** + 7  $\mu$ M CK2 $\alpha$

~~~~~ 0.5 mM **1**

319

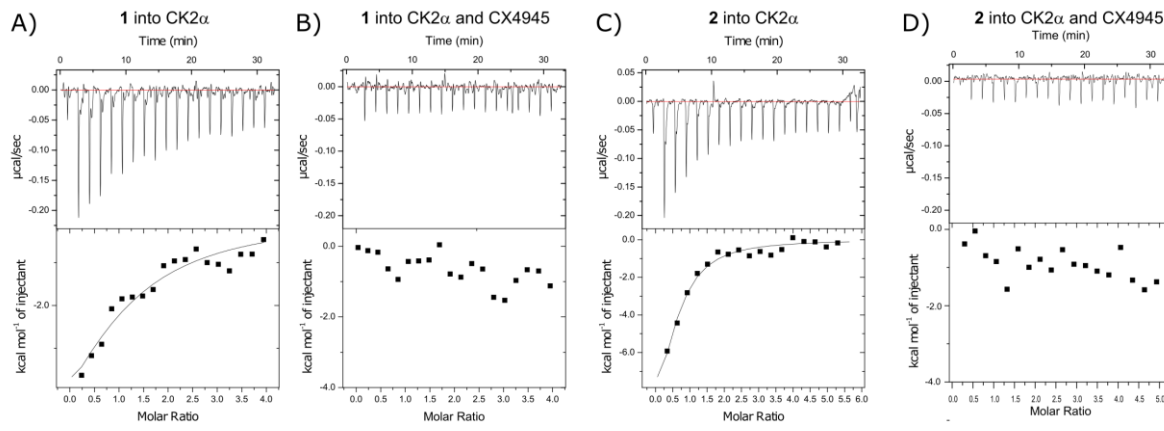
320

321 **Figure 5. Ligand-based NMR experiments to detect binding of 1 to CK2 α and competition by**
322 **CX4945.** All panels are overlays of spectra recorded in the presence (black) and absence (green) of
323 CK2 α . (A) Saturation Transfer Difference (STD) ^1H spectra of **1** (i) in the absence of **CX4945**, and (ii) in
324 the presence of 50 μM **CX4945**. (B) WaterLOGSY spectra of **1** (i) in the absence of **CX4945**, and (ii) in
325 the presence of 50 μM **CX4945** (ii). (C) Relaxation-edited (CPMG) ^1H spectra of **1** (i) in the absence of
326 **CX4945**, and (ii) in the presence of 50 μM **CX4945** (ii). (NB: the signals at ca. 7.7 ppm are in fact two
327 overlapping doublets and therefore small changes to either chemical shift results in an apparent
328 change to the multiplet structure.)

329 To further confirm the validity of our results, we repeated the CPMG NMR study using the lower
330 affinity ligands **3**, **5** and **CAM4066** as competitors (SI Fig. 13). **3** is a small, low affinity ligand in the
331 ATP site and as such it is less likely to have an allosteric affect that might prevent binding at the
332 adjacent Site A – an argument that could explain inhibition of binding to **1** in the presence of
333 **CX4945**. Therefore, the reduction in the binding of **1** in the presence of **3** (SI Fig. 13B) is a more
334 convincing proof that **1** is binding in the ATP site. **CAM4066** links the ATP site and the αD site and, as
335 predicted, reduces the binding of **1** to CK2 α (SI Fig. 13C). To rule out binding of **1** to the αD site, we
336 have also used **5**, an optimized fragment with high affinity for the αD site. This should not prevent
337 binding in the ATP site. Indeed, ligands similar to **5** have been shown to bind simultaneously with
338 ATP site fragments by X-ray crystallography (PDB:6EHK)²⁶. As predicted, and unlike with **CX4945**, **3**
339 and **CAM4066**, the αD site ligand **5** has no effect on the binding of **1** to CK2 α (SI Fig. 13D). Similar
340 CPMG and STD NMR experiments were performed with the CK2 α KKK/AAA mutant with the same
341 outcomes (SI Fig. 14 and 15). These results further demonstrate that **1** binds in the ATP site.

342 Isothermal titration calorimetry
343 As a final confirmation, we have used isothermal titration calorimetry to determine affinities of **1**
344 and **2** to CK2 α and to evaluate the effect of competing ligands and CK2 α mutations. This process has
345 been successfully used to verify the binding site of novel CK2 inhibitors that bind in the αD site²⁶.
346 The affinities of compounds **1** and **2** for CK2 α were determined to be 22 μM and 2.2 μM respectively
347 (Fig. 6A and C). When the same experiments were performed in the presence of saturating
348 concentrations of **CX4945**, no binding of either compound to CK2 α was observed (Fig. 6B and 6D).
349 This observation is in line with all our previous data and suggests that compounds **1** and **2** bind in the
350 same site as **CX4945**. We also performed the experiment with **2** in the presence of **CAM4066**, which
351 competes with ATP, but uses only a small benzoic acid moiety to interact with the ATP site, deriving
352 most of its binding energy from the αD pocket. **CAM4066** abolished the binding of **2** to CK2 α (SI Fig.
353 16). In the modelling of the binding of **1** and **2** reported previously^{35,36}, Lys74 was proposed to form a
354 vital part of the binding site and to interact with the carboxylic acid of **1** and **2**. Therefore, mutations

355 to this residue should reduce the affinity of **1** and **2** for CK2 α . To test this, we repeated the ITC
356 experiments using the construct CK2 α KKK/AAA, in which three adjacent lysine residues (Lys74-76)
357 have been mutated to alanine. These mutations had a negligible effect on the affinity of **1** or **2** for
358 CK2 α as we determined near identical affinities of 27 μ M and 3.3 μ M, respectively (SI Fig. 16). The
359 binding of **1** and **2** to CK2 α KKK/AAA was also fully inhibited by the presence of **CX4945** and
360 **CAM4066** respectively (SI Fig. 16). These results are further evidence that the ATP site, not the
361 proposed allosteric site, is the primary binding site for **1** and **2**.



363 **Figure 6. ITC measurement of binding of **1** and **2** to CK2 α .** (A) Titration of **1** into 10 μ M CK2 α
364 Titration of **2** into 10 μ M CK2 α . (B) Titration of **1** into 10 μ M CK2 α Titration of **2** into 10 μ M CK2 α in
365 the presence of **CX4945** (C) Titration of **2** into 20 μ M CK2 α . (D) Titration of **2** into 20 μ M CK2 α in the
366 presence of 100 μ M **CX4945**.

367 **Discussion**

368 We present compelling and consistent evidence that **1** and **2** bind in the ATP site of CK2 α , not in Site
369 A, as was previously proposed.^{35,36} We see no evidence for binding in Site A. This is as expected,
370 based on our analysis of the structural data of similar kinase inhibitors. In the original study of Series
371 A,³⁶ five main pieces of evidence were used to verify a novel binding mode. This evidence included:
372 competitive native mass spectroscopy studies, ligand-based NMR, thermal shift analysis and
373 biochemical assays. While we were preparing this manuscript for publication, the Niefind group
374 published their analysis of the same series of compounds, which also showed binding to the ATP site
375 by X-ray crystallography.⁶⁹ While they have not done other biophysical analyses on the binding, they
376 do show by enzymatic assay that these inhibitors are ATP competitive, consistent with our data.

377 One of the cornerstones of the theory of allosteric inhibition was the observation that that **CX4945**
378 binds CK2 α simultaneously with **1**, and that **1** competes with inositol hexaphosphate (IP₆, phytic
379 acid), shown by mass spectrometry. The data presented indicate that at least three molecules of **1**
380 bind to CK2 α . In the presence of **CX4945** this is reduced to two binding sites, but no data were

381 presented to confirm the identity of these sites in which **1** was binding when it bound
382 simultaneously with **CX4945** (for example mutational studies combined with native mass
383 spectrometry). Some of these sites are expected to be non-specific, low affinity sites and the mass
384 spectrometric data does not confirm which is the primary binding site of **1**. The first evidence
385 presented for the location of the binding site of these compounds is the observation that in the
386 presence of **1** the complex between IP₆ and CK2 α is not observed in the native mass spectra. This led
387 to the theory that **1** binds in the proposed site as a crystal structure was published by Lee et al
388 (PDB:3W8L)⁷⁰ of IP₆ apparently binding to CK2 α in this site. However, the binding site of IP₆
389 presented in that crystal structure is more controversial than is discussed in the publication.⁷⁰ In this
390 structure, IP₆ is found at a crystal contact where half of the site is composed of residues from a
391 symmetry related CK2 α molecule in the crystal lattice (SI Fig. 17). Therefore, IP₆ could in theory bind
392 to both these sites. From this crystal structure the binding site could be located around Lys74 or
393 His276. However, as the site is only fully formed in a crystal lattice (SI Fig. 17), IP₆ may not in actual
394 fact bind to CK2 α at either of these sites in solution. IP₆ is also seen to bind weakly at a site centered
395 on His236 in several other crystal structures (PDB:5OQU, 5ORJ, 5MPJ, 5CVH)^{26,27,60}. The native mass
396 spectrometric competition studies with **CX4945** or IP₆ do not therefore unambiguously confirm the
397 binding mode of **1**.

398 Another cornerstone of the allosteric site binding was the observation of the binding by ligand-based
399 NMR and simultaneous detection of **CX4945** binding, interpreted as lack of competition. As
400 discussed before, a high affinity ligand like **CX4945**, with slow dissociation rate should not yield
401 detectable signal in these experiments. The binding of **CX4945** observed in those STD experiments is
402 however more likely to be due to an artefact in the experimental setup. This could be through a
403 number of mechanisms including aggregation of the ligand or binding to non-specific lower affinity
404 binding sites outside the ATP site.⁷¹ These lower affinity sites would have higher on/off rates than
405 the ATP site and therefore show a larger signal in the STD spectrum. Non-specific and low affinity
406 sites can have a confusing influence on competition studies. This is a particular problem with the
407 NMR studies as ligand-detected NMR is optimized for studying low affinity sites and requires ligands
408 with rapid on/off rates in order for the signal (and therefore binding) to be observed. Therefore,
409 blocking the primary (high affinity) site may not remove the binding signal arising from other sites.
410 The competition studies in the original papers were done at 500 μ M ligand concentration, well
411 beyond the observed affinities or K_s of **1** and **2** and in a range where non-specific binding would be
412 more likely to occur.^{35,36} The binding signals observed for **CX4945** in the STD spectra cast some doubt
413 on the conclusions drawn about the simultaneous binding of **1** and **CX4945**. This is because the
414 signals observed for **CX4945** cannot be due to binding in the ATP site as the dissociation rate for this

415 site is too slow. The major difference between our experimental system and the system reported in
416 the literature is the DMSO content. In brief, in the procedure reported here stocks of **1** and **2** were
417 made in d₆-DMSO and diluted 20-fold in the buffer. This was done to ensure the ligands were fully
418 soluble in the experiment and led to a final d₆-DMSO content of 5% (which was also used to provide
419 the field-frequency lock signal). When we first attempted to run the experiment without DMSO, we
420 observed precipitation of the ligands. As aggregation can lead to false positives in STD experiments
421 it was decided to use DMSO in all our experiments.⁷¹ However, in the original experiment D₂O was
422 used for the lock and no DMSO was used to solubilise the ligand. The difference in the solvent
423 conditions may mean that **1** and **2** were closer to the limits of their solubility in the original
424 experiments and thus more likely to form aggregates. Aggregates are common causes of false
425 positives in biochemical assays and are often missed as they may not be easily visible to the naked
426 eye. These aggregates may lead to the signals observed in the STD for **CX4945** and **1**.

427 The biochemical assays performed previously showed that the compounds exhibited mixed mode
428 non-competitive behavior and led to the understandable conclusion that they do not bind in the ATP
429 site. However, this is contradictory to the binding mode we see in the crystal structures. A proposed
430 explanation for the non-competitive inhibition observed in the assay comes from the thermal
431 stability data also presented in the original paper.³⁵ The data show that the thermal stability of the
432 proteins decreases in the presence of **1** and **2**. This thermal de-stabilization could be due to a
433 number of different mechanisms caused by specific and non-specific effects. These mechanisms
434 include; breaking up of protein complexes by specific binding to the protein; binding to the unfolded
435 or partially unfolded protein; the formation of aggregates that bind the protein and unfold it and
436 specific binding that traps the protein in a less stable conformation⁷²⁻⁷⁵.

437 It is impossible that the first mechanism is operating in this example as CK2 α is present as a
438 monomer. The other mechanisms however may explain the conflicting results presented. All
439 proteins exist in an equilibrium between the native and unfolded form of the protein.⁷⁶ For the
440 majority of ligands, the ligand binds to the native form of the protein which stabilizes the folded
441 form leading to a positive thermal shift. If the ligand binds to the unfolded or partially unfolded form
442 of the protein and stabilize the unfolded form this could lead to a destabilization of the protein. This
443 would in turn lead to a decrease in the T_m . Binding to the unfolded protein can occur by two
444 mechanisms, the first mechanism is by the formation of colloidal aggregates of the small molecules,
445 onto which the protein would then be sequestered.⁷⁵ The aggregates are hydrophobic and
446 preferentially bind the unfolded or partially unfolded form of the protein where the hydrophobic
447 core is exposed. Therefore, a negative shift in the T_m is observed. This is one of the most common
448 forms of non-specific inhibition that plague biochemical assays and would be seen in assays as

449 noncompetitive inhibition. The second mechanism occurs when the ligand monomers bind to a
450 partially unfolded or fully unfolded form of the protein stabilizing that form. It may be possible for
451 the binding to the partially unfolded form to be a specific form of inhibition.

452 Modelling experiments proposed Site A as the binding site for **1** and **2** (SI Fig. 8)³⁵. We have
453 accumulated extensive evidence that these compounds bind in the ATP site. However, Site A as a
454 general ligand binding site has been verified by our structures of ADP and GDP bound in this
455 location. This suggests that Site A could be utilized for the development of novel inhibitors of CK2 α
456 and it also demonstrates that this site is accessible for ligand binding in our crystal forms. If this site
457 were to be successfully targeted by inhibitors, it would require extensive structural and biochemical
458 validation to confirm that compounds are really binding in the new site and not in one of the several
459 known small molecule binding sites in CK2 α .

460 We believe that the data we have presented here leads to the conclusion that the compounds
461 represented by **1** and **2** bind to the ATP site and will inhibit CK2 α via an orthosteric, ATP-competitive
462 mechanism. This diverse set of data pointing to **1** and **2** binding at the ATP site includes multiple
463 crystal structures, competitive ITC studies, competitive NMR studies, H/D exchange mass
464 spectrometry and computational analyses of the ligand structures. We also believe that the evidence
465 presented previously in support of an allosteric mode of inhibition for these compounds may have
466 been distorted by non-specific binding of the compounds to CK2 α , which in turn affected the
467 interpretation of competition data with **CX4945**.

468 Acknowledgements:
469 We would like to thank Dr Glyn Williams and Teodors Pantelejevs for their critical comments on the
470 manuscript. We are grateful for Diamond Light Source for access to beamlines i04, i04-1 and i24
471 (proposals: mx9537, mx14043, mx18548). We thank the X-ray Crystallographic and Biophysics
472 Facilities for access to instrumentation. We thank Apollo Therapeutics that funds our CK2 α inhibitor
473 development project for allowing the use of the data on CX4945 binding kinetics for this publication.
474 The work in the D'Arcy group was funded by the NIH National Institute of General Medical Sciences
475 (GM133751) and start-up funds to S. D'Arcy.

476 Structural coordinates in Protein Data Bank
477 6YPG (CK2 α in complex with **2**), 6YPH (CK2 α in complex with **2**), 6YPJ (CK2 α in complex with **1**), 6YPK
478 (CK2 α in complex with **GDP**), 6YPN (CK2 α in complex with **ATP**).

479 Bibliography
480 (1) Roskoski, R. Properties of FDA-Approved Small Molecule Protein Kinase Inhibitors.
481 *Pharmacological Research*. Academic Press June 2019, pp 19–50.

482 https://doi.org/10.1016/j.phrs.2019.03.006.

483 (2) Wu, P.; Nielsen, T. E.; Clausen, M. H. FDA-Approved Small-Molecule Kinase Inhibitors. *Trends Pharmacol. Sci.* **2015**, 36 (7), 422–439. <https://doi.org/10.1016/j.tips.2015.04.005>.

484 (3) Smyth, L. A.; Collins, I. Measuring and Interpreting the Selectivity of Protein Kinase Inhibitors. *J. Chem. Biol.* **2009**, 2 (3), 131–151. <https://doi.org/10.1007/s12154-009-0023-9>.

485 (4) Davis, M. I.; Hunt, J. P.; Herrgard, S.; Ciceri, P.; Wodicka, L. M.; Pallares, G.; Hocker, M.; Treiber, D. K.; Zarrinkar, P. P. Comprehensive Analysis of Kinase Inhibitor Selectivity. *Nat. Biotechnol.* **2011**, 29 (11), 1046–1051. <https://doi.org/10.1038/nbt.1990>.

486 (5) Drag, M.; Salvesen, G. S. Emerging Principles in Protease-Based Drug Discovery. *Nat. Rev. Drug Discov.* **2010**, 9 (9), 690–701. <https://doi.org/10.1038/nrd3053>.

487 (6) Bain, J.; Plater, L.; Elliott, M.; Shpiro, N.; Hastie, C. J.; McLauchlan, H.; Klevernic, I.; Arthur, J. S. C.; Alessi, D. R.; Cohen, P. The Selectivity of Protein Kinase Inhibitors: A Further Update. *Biochem. J.* **2007**, 408 (3), 297–315. <https://doi.org/10.1042/BJ20070797>.

488 (7) Bain, J.; McLauchlan, H.; Elliott, M.; Cohen, P. The Specificities of Protein Kinase Inhibitors: An Update. *Biochem. J.* **2003**, 371 (1), 199–204. <https://doi.org/10.1042/BJ20021535>.

489 (8) Tarcsey, Á.; Keserú, G. M. Contributions of Molecular Properties to Drug Promiscuity. *Journal of Medicinal Chemistry*. American Chemical Society March 2013, pp 1789–1795. <https://doi.org/10.1021/jm301514n>.

490 (9) Bowes, J.; Brown, A. J.; Hamon, J.; Jarolimek, W.; Sridhar, A.; Waldron, G.; Whitebread, S. Reducing Safety-Related Drug Attrition: The Use of in Vitro Pharmacological Profiling. *Nature Reviews Drug Discovery*. Nat Rev Drug Discov December 2012, pp 909–922. <https://doi.org/10.1038/nrd3845>.

491 (10) Lu, X.; Smaill, J. B.; Ding, K. New Promise and Opportunities for Allosteric Kinase Inhibitors. *Angew. Chemie Int. Ed.* **2019**. <https://doi.org/10.1002/anie.201914525>.

492 (11) Lebakken, C. S.; Reichling, L. J.; Ellefson, J. M.; Riddle, S. M. Detection of Allosteric Kinase Inhibitors by Displacement of Active Site Probes. *J. Biomol. Screen.* **2012**, 17 (6), 813–821. <https://doi.org/10.1177/1087057112439889>.

493 (12) Fasano, M.; Della Corte, C. M.; Califano, R.; Capuano, A.; Troiani, T.; Martinelli, E.; Ciardiello, F.; Morgillo, F. Type III or Allosteric Kinase Inhibitors for the Treatment of Non-Small Cell Lung Cancer. *Expert Opin. Investig. Drugs* **2014**, 23 (6), 809–821.

512 https://doi.org/10.1517/13543784.2014.902934.

513 (13) Wu, P.; Clausen, M. H.; Nielsen, T. E. Allosteric Small-Molecule Kinase Inhibitors.
514 *Pharmacology and Therapeutics*. Elsevier Inc. December 2015, pp 59–68.
515 https://doi.org/10.1016/j.pharmthera.2015.10.002.

516 (14) McGovern, S. L.; Shoichet, B. K. Kinase Inhibitors: Not Just for Kinases Anymore. *J. Med.*
517 *Chem.* **2003**, *46* (8), 1478–1483. https://doi.org/10.1021/jm020427b.

518 (15) Ahmad, K. A.; Wang, G.; Slaton, J.; Unger, G.; Ahmed, K. Targeting CK2 for Cancer Therapy.
519 *Anticancer. Drugs* **2005**, *16* (10), 1037–1043.

520 (16) Ruzzene, M.; Pinna, L. A. Addiction to Protein Kinase CK2: A Common Denominator of Diverse
521 Cancer Cells? *Biochim. Biophys. Acta - Proteins Proteomics* **2010**, *1804* (3), 499–504.
522 https://doi.org/10.1016/j.bbapap.2009.07.018.

523 (17) Panicker, R. C.; Chattopadhyaya, S.; Coyne, A. G.; Srinivasan, R. Allosteric Small-Molecule
524 Serine/Threonine Kinase Inhibitors. *Adv. Exp. Med. Biol.* **2019**, *1163*, 253–278.
525 https://doi.org/10.1007/978-981-13-8719-7_11.

526 (18) Kim, H.; Choi, K.; Kang, H.; Lee, S. Y.; Chi, S. W.; Lee, M. S.; Song, J.; Im, D.; Choi, Y.; Cho, S.
527 Identification of a Novel Function of CX-4945 as a Splicing Regulator. *PLoS One* **2014**, *9* (4), 1–
528 8. https://doi.org/10.1371/journal.pone.0094978.

529 (19) Meggio, F.; Pinna, L. a. One-Thousand-and-One Substrates of Protein Kinase CK2? *FASEB J.*
530 **2003**, *17* (3), 349–368. https://doi.org/10.1096/fj.02-0473rev.

531 (20) Cozza, G.; Pinna, L. a; Moro, S. Protein Kinase CK2 Inhibitors: A Patent Review. *Expert Opin.*
532 *Ther. Pat.* **2012**, *22* (9), 1081–1097. https://doi.org/10.1517/13543776.2012.717615.

533 (21) Quotti Tubi, L.; Gurrieri, C.; Brancalion, A.; Bonaldi, L.; Bertorelle, R.; Manni, S.; Pavan, L.;
534 Lessi, F.; Zambello, R.; Trentin, L.; Adami, F.; Ruzzene, M.; Pinna, L. A.; Semenzato, G.; Piazza,
535 F. Inhibition of Protein Kinase CK2 with the Clinical-Grade Small ATP-Competitive Compound
536 CX-4945 or by RNA Interference Unveils Its Role in Acute Myeloid Leukemia Cell Survival, P53-
537 Dependent Apoptosis and Daunorubicin-Induced Cytotoxicity. *J. Hematol. Oncol.* **2013**, *6* (1),
538 78. https://doi.org/10.1186/1756-8722-6-78.

539 (22) Sarno, S.; Salvi, M.; Battistutta, R.; Zanotti, G.; Pinna, L. A. Features and Potentials of ATP-Site
540 Directed CK2 Inhibitors. In *Biochimica et Biophysica Acta - Proteins and Proteomics*; Biochim
541 Biophys Acta, 2005; Vol. 1754, pp 263–270. https://doi.org/10.1016/j.bbapap.2005.07.043.

542 (23) Mazzorana, M.; Pinna, L. A.; Battistutta, R. A Structural Insight into CK2 Inhibition. *Mol. Cell. Biochem.* **2008**, 316 (1–2), 57–62. <https://doi.org/10.1007/s11010-008-9822-5>.

543 (24) Kufareva, I.; Bestgen, B.; Brear, P.; Prudent, R.; Laudet, B.; Moucadel, V.; Ettaoussi, M.; Sautel, C. F.; Krimm, I.; Engel, M.; Filhol, O.; Borgne, M. Le; Lomberget, T.; Cochet, C.; Abagyan, R. Discovery of Holoenzyme-Disrupting Chemicals as Substrate-Selective CK2 Inhibitors. *Sci. Rep.* **2019**, 9 (1), 15893. <https://doi.org/10.1038/s41598-019-52141-5>.

544 (25) Brear, P.; De Fusco, C.; Hadje Georgiou, K.; Francis-Newton, N. J.; Stubbs, C. J.; Sore, H. F.; Venkitaraman, A. R.; Abell, C.; Spring, D. R.; Hyvönen, M. Specific Inhibition of CK2 α from an Anchor Outside the Active Site. *Chem. Sci.* **2016**, 7 (11), 6839–6845. <https://doi.org/10.1039/C6SC02335E>.

545 (26) Iegre, J.; Brear, P.; De Fusco, C.; Yoshida, M.; Mitchell, S. L.; Rossmann, M.; Carro, L.; Sore, H. F.; Hyvönen, M.; Spring, D. R. Second-Generation CK2 α Inhibitors Targeting the Ad Pocket. *Chem. Sci.* **2018**, 9 (11), 3041–3049. <https://doi.org/10.1039/c7sc05122k>.

546 (27) De Fusco, C.; Brear, P.; Iegre, J.; Georgiou, K. H.; Sore, H. F.; Hyvönen, M.; Spring, D. R. A Fragment-Based Approach Leading to the Discovery of a Novel Binding Site and the Selective CK2 Inhibitor CAM4066. *Bioorg. Med. Chem.* **2017**, 25 (13), 3471–3482. <https://doi.org/10.1016/j.bmc.2017.04.037>.

547 (28) Guerra, B.; Hochscherf, J.; Jensen, N. B.; Issinger, O.-G. Identification of a Novel Potent, Selective and Cell Permeable Inhibitor of Protein Kinase CK2 from the NIH/NCI Diversity Set Library. *Mol. Cell. Biochem.* **2015**. <https://doi.org/10.1007/s11010-015-2433-z>.

548 (29) Prins, R. C.; Burke, R. T.; Tyner, J. W.; Druker, B. J.; Loriaux, M. M.; Spurgeon, S. E. CX-4945, a Selective Inhibitor of Casein Kinase-2 (CK2), Exhibits Anti-Tumor Activity in Hematologic Malignancies Including Enhanced Activity in Chronic Lymphocytic Leukemia When Combined with Fludarabine and Inhibitors of the B-Cell Receptor Pathway. *Leukemia* **2013**, 27 (10), 2094–2096. <https://doi.org/10.1038/leu.2013.228>.

549 (30) Dowling, J. E.; Alimzhanov, M.; Bao, L.; Chuaqui, C.; Denz, C. R.; Jenkins, E.; Larsen, N. A.; Lyne, P. D.; Pontz, T.; Ye, Q.; Holdgate, G. A.; Snow, L.; O'Connell, N.; Ferguson, A. D. Potent and Selective CK2 Kinase Inhibitors with Effects on Wnt Pathway Signaling in Vivo. *ACS Med. Chem. Lett.* **2016**, 7 (3), 300–305. <https://doi.org/10.1021/acsmmedchemlett.5b00452>.

550 (31) Götz, C.; Gratz, A.; Kucklaender, U.; Jose, J. TF — A Novel Cell-Permeable and Selective Inhibitor of Human Protein Kinase CK2 Induces Apoptosis in the Prostate Cancer Cell Line

573 LNCaP. *Biochim. Biophys. Acta - Gen. Subj.* **2012**, 1820 (7), 970–977.
574 <https://doi.org/10.1016/j.bbagen.2012.02.009>.

575 (32) Pierre, F.; Chua, P. C.; O'Brien, S. E.; Siddiqui-Jain, A.; Bourbon, P.; Haddach, M.; Michaux, J.;
576 Nagasawa, J.; Schwaebel, M. K.; Stefan, E.; Vialettes, A.; Whitten, J. P.; Chen, T. K.; Darjania, L.;
577 Stansfield, R.; Bliesath, J.; Drygin, D.; Ho, C.; Omori, M.; Proffitt, C.; Streiner, N.; Rice, W. G.;
578 Ryckman, D. M.; Anderes, K. Pre-Clinical Characterization of CX-4945, a Potent and Selective
579 Small Molecule Inhibitor of CK2 for the Treatment of Cancer. *Mol. Cell. Biochem.* **2011**, 356
580 (1–2), 37–43. <https://doi.org/10.1007/s11010-011-0956-5>.

581 (33) Iegre, J.; Brear, P.; Baker, D. J.; Tan, Y. S.; Atkinson, E. L.; Sore, H. F.; O' Donovan, D. H.;
582 Verma, C. S.; Hyvönen, M.; Spring, D. R. Efficient Development of Stable and Highly
583 Functionalised Peptides Targeting the CK2 α /CK2 β Protein-Protein Interaction. *Chem. Sci.*
584 **2019**, 10 (19), 5056–5063. <https://doi.org/10.1039/c9sc00798a>.

585 (34) Brear, P.; North, A.; Iegre, J.; Georgiou, K. H.; Lubin, A.; Carro, L.; Green, W.; Sore, H. F.;
586 Hyvönen, M.; Spring, D. R. Bioorganic & Medicinal Chemistry Novel Non-ATP Competitive
587 Small Molecules Targeting the CK2 α / β Interface. *Bioorg. Med. Chem.* **2018**, 26 (11), 3016–
588 3020. <https://doi.org/10.1016/j.bmc.2018.05.011>.

589 (35) Bestgen, B.; Kufareva, I.; Seetoh, W.; Abell, C.; Hartmann, R. W.; Abagyan, R.; Le Borgne, M.;
590 Filhol, O.; Cochet, C.; Lomberget, T.; Engel, M. 2-Aminothiazole Derivatives as Selective
591 Allosteric Modulators of the Protein Kinase CK2. 2. Structure-Based Optimization and
592 Investigation of Effects Specific to the Allosteric Mode of Action. *J. Med. Chem.* **2019**, 62 (4),
593 1817–1836. <https://doi.org/10.1021/acs.jmedchem.8b01765>.

594 (36) Bestgen, B.; Krimm, I.; Kufareva, I.; Kamal, A. A. M.; Seetoh, W. G.; Abell, C.; Hartmann, R. W.;
595 Abagyan, R.; Cochet, C.; Le Borgne, M.; Engel, M.; Lomberget, T. 2-Aminothiazole Derivatives
596 as Selective Allosteric Modulators of the Protein Kinase CK2. 1. Identification of an Allosteric
597 Binding Site. *J. Med. Chem.* **2019**, 62 (4), 1803–1816.
598 <https://doi.org/10.1021/acs.jmedchem.8b01766>.

599 (37) Ngoei, K. R. W.; Langendorf, C. G.; Ling, N. X. Y.; Hoque, A.; Varghese, S.; Camerino, M. A.;
600 Walker, S. R.; Bozikis, Y. E.; Dite, T. A.; Ovens, A. J.; Smiles, W. J.; Jacobs, R.; Huang, H.; Parker,
601 M. W.; Scott, J. W.; Rider, M. H.; Foitzik, R. C.; Kemp, B. E.; Baell, J. B.; Oakhill, J. S. Structural
602 Determinants for Small-Molecule Activation of Skeletal Muscle AMPK Alpha 2 Beta 2 Gamma
603 1 by the Glucose Importer SC4. *Cell Chem Biol* **2018**, 25, 728-737.e9.
604 <https://doi.org/10.2210/PDB6B1U/PDB>.

605 606 607 608 (38) Guerra, B.; Rasmussen, T. D.; Schnitzler, A.; Jensen, H. H.; Boldyreff, B. S.; Miyata, Y.;
Marcussen, N.; Niefeld, K.; Issinger, O. G. Protein Kinase CK2 Inhibition Is Associated with the
Destabilization of HIF-1 Alpha in Human Cancer Cells. *Cancer Lett.* **2015**, *356*, 751–761.
<https://doi.org/10.2210/PDB4RLK/PDB>.

609 610 611 612 (39) Gazzard, L.; Appleton, B.; Chapman, K.; Chen, H.; Clark, K.; Drobnick, J.; Goodacre, S.;
Halladay, J.; Lyssikatos, J.; Schmidt, S.; Sideris, S.; Wiesmann, C.; Williams, K.; Wu, P.; Yen, I.;
Malek, S. Discovery of the 1,7-Diazacarbazole Class of Inhibitors of Checkpoint Kinase 1.
Bioorg. Med. Chem. Lett. **2014**, *24*, 5704–5709. <https://doi.org/10.2210/PDB4QYE/PDB>.

613 614 (40) Kang, Y. N.; Stuckey, J. A.; Chang, P.; Russell, A. J. Crystal Structure of the CHK1. *TO BE Publ.*
<https://doi.org/10.2210/PDB4FT0/PDB>.

615 616 617 618 619 (41) Lawrence, H. R.; Martin, M. P.; Luo, Y.; Pireddu, R.; Yang, H.; Gevariya, H.; Ozcan, S.; Zhu, J.-Y.;
Kendig, R.; Rodriguez, M.; Elias, R.; Cheng, J. Q.; Sebti, S. M.; Schonbrunn, E.; Lawrence, N. J.
Development of O-Chlorophenyl Substituted Pyrimidines as Exceptionally Potent Aurora
Kinase Inhibitors. *J. Med. Chem.* **2012**, *55* (17), 7392–7416.
<https://doi.org/10.1021/jm300334d>.

620 621 622 623 (42) Xiao, B.; Sanders, M. J.; Carmena, D.; Bright, N. J.; Haire, L. F.; Underwood, E.; Patel, B. R.;
Heath, R. B.; Walker, P. A.; Hallen, S.; Giordanetto, F.; Martin, S. R.; Carling, D.; Gamblin, S. J.
Structural Basis of Ampk Regulation by Small Molecule Activators. *Nat. Commun.* **2013**, *4*,
3017. <https://doi.org/10.2210/PDB4CFE/PDB>.

624 625 626 (43) Xue, Y.; Wan, P. T.; Hillertz, P.; Schweikart, F.; Zhao, Y.; Wissler, L.; Dekker, N. X-Ray Structural
Analysis of Tau-Tubulin Kinase 1 and Its Interactions with Small Molecular Inhibitors.
ChemMedChem **2013**, *8*, 1846. <https://doi.org/10.2210/PDB4BTM/PDB>.

627 628 629 630 (44) Elkins, J. M.; Muniz, J. R. C.; Tan, I.; Leung, T.; Lafanechere, L.; Prudent, R.; Abdul Azeez, K.;
Szklarz, M.; Phillips, C.; Wang, J.; von Delft, F.; Bountra, C.; Edwards, A.; Knapp, S. Cdc42
Binding Protein Kinase Alpha (Mrck Alpha). *TO BE Publ.*
<https://doi.org/10.2210/PDB4AW2/PDB>.

631 632 633 634 (45) Martin, M. P.; Zhu, J. Y.; Lawrence, H. R.; Pireddu, R.; Luo, Y.; Alam, R.; Ozcan, S.; Sebti, S. M.;
Lawrence, N. J.; Schönbunn, E. A Novel Mechanism by Which Small Molecule Inhibitors
Induce the DFG Flip in Aurora A. *ACS Chem. Biol.* **2012**, *7* (4), 698–706.
<https://doi.org/10.1021/cb200508b>.

635 (46) Battistutta, R.; Cozza, G.; Pierre, F.; Papinutto, E.; Lolli, G.; Sarno, S.; O'Brien, S. E.; Siddiqui-

636 Jain, A.; Haddach, M.; Anderes, K.; Ryckman, D. M.; Meggio, F.; Pinna, L. a. Unprecedented
637 Selectivity and Structural Determinants of a New Class of Protein Kinase CK2 Inhibitors in
638 Clinical Trials for the Treatment of Cancer. *Biochemistry* **2011**, *50* (39), 8478–8488.
639 <https://doi.org/10.1021/bi2008382>.

640 (47) Ferguson, A. D.; Sheth, P. R.; Basso, A. D.; Paliwal, S.; Gray, K.; Fischmann, T. O.; Le, H. V.
641 Structural Basis of CX-4945 Binding to Human Protein Kinase CK2. *FEBS Lett.* **2011**, *585* (1),
642 104–110. <https://doi.org/10.1016/j.febslet.2010.11.019>.

643 (48) Iegre, J.; Brear, P.; Baker, D. J.; Tan, Y. S.; Atkinson, E. L.; Sore, H. F.; O' Donovan, D. H.;
644 Verma, C. S.; Hyvonen, M.; Spring, D. R. Efficient Development of Stable and Highly
645 Functionalised Peptides Targeting the CK2 Alpha /CK2 Beta Protein-Protein Interaction. *Chem
646 Sci* **2019**, *10*, 5056–5063. <https://doi.org/10.2210/PDB6Q38/PDB>.

647 (49) Filippakopoulos, P.; Rellos, P.; Fedorov, O.; Niesen, F.; Pike, A. C. W.; Pilka, E. S.; von Delft, F.;
648 Arrowsmith, C. H.; Edwards, A. M.; Weigelt, J.; Knapp, S. Crystal Structure of Human Death
649 Associated Protein Kinase 3 (DAPK3) in Complex with an Imidazo-Pyridazine Ligand. *TO BE
650 Publ.* <https://doi.org/10.2210/PDB3BQR/PDB>.

651 (50) Pierce, A. C.; Jacobs, M.; Stuver-Moody, C. Docking Study Yields Four Novel Inhibitors of the
652 Protooncogene Pim-1 Kinase. *J. Med. Chem.* **2008**, *51*, 1972–1975.
653 <https://doi.org/10.2210/PDB3BGZ/PDB>.

654 (51) Hou, Z.; Nakanishi, I.; Kinoshita, T.; Takei, Y.; Yasue, M.; Misu, R.; Suzuki, Y.; Nakamura, S.;
655 Kure, T.; Ohno, H.; Murata, K.; Kitaura, K.; Hirasawa, A.; Tsujimoto, G.; Oishi, S.; Fujii, N.
656 Structure-Based Design of Novel Potent Protein Kinase CK2 (CK2) Inhibitors with Phenyl-Azole
657 Scaffolds. *J. Med. Chem.* **2012**, *55* (6), 2899–2903. <https://doi.org/10.1021/jm2015167>.

658 (52) Whelligan, D. K.; Solanki, S.; Taylor, D.; Thomson, D. W.; Cheung, K. M.; Boxall, K.; Mas-Droux,
659 C.; Barillari, C.; Burns, S.; Grummitt, C. G.; Collins, I.; Van Montfort, R. L.; Aherne, G. W.;
660 Bayliss, R.; Hoelder, S. Aminopyrazine Inhibitors Binding to an Unusual Inactive Conformation
661 of the Mitotic Kinase Nek2: Sar and Structural Characterization. *J. Med. Chem.* **2010**, *53*, 7682.
662 <https://doi.org/10.2210/PDB2XK4/PDB>.

663 (53) Pike, A. C. W.; Savitsky, P.; Fedorov, O.; Krojer, T.; Ugochukwu, E.; von Delft, F.; Gileadi, O.;
664 Edwards, A.; Arrowsmith, C. H.; Weigelt, J.; Bountra, C.; Knapp, S. Structure of Human Serine-
665 Arginine-Rich Protein- Specific Kinase 2 (Srpk2) Bound to Purvalanol B. *TO BE Publ.*
666 <https://doi.org/10.2210/PDB2X7G/PDB>.

667 (54) Dodson, C. A.; Kosmopoulou, M.; Richards, M. W.; Atrash, B.; Bavetsias, V.; Blagg, J.; Bayliss,
668 R. Crystal Structure of an Aurora-A Mutant That Mimics Aurora-B Bound to MIn8054: Insights
669 Into Selectivity and Drug Design. *Biochem.J.* **2010**, *427*, 19.
670 <https://doi.org/10.2210/PDB2WTV/PDB>.

671 (55) Richards, M. W.; O'Regan, L.; Mas-Droux, C.; Blot, J. M.; Cheung, J.; Hoelder, S.; Fry, A. M.;
672 Bayliss, R. An Autoinhibitory Tyrosine Motif in the Cell-Cycle- Regulated Nek7 Kinase Is
673 Released Through Binding of Nek9. *Mol.Cell* **2009**, *36*, 560.
674 <https://doi.org/10.2210/PDB2WQO/PDB>.

675 (56) Tong, Y.; Claiborne, A.; Stewart, K. D.; Park, C.; Kovar, P.; Chen, Z.; Credo, R. B.; Gu, W. Z.;
676 Gwaltney, S. L.; Judge, R. A.; Zhang, H.; Rosenberg, S. H.; Sham, H. L.; Sowin, T. J.; Lin, N. H.
677 Discovery of 1,4-Dihydroindeno[1,2-c]Pyrazoles as a Novel Class of Potent and Selective
678 Checkpoint Kinase 1 Inhibitors. *Bioorg.Med.Chem.* **2007**, *15*, 2759–2767.
679 <https://doi.org/10.2210/PDB2E9O/PDB>.

680 (57) Pattanayek, R.; Egli, M. Protein-Protein Interactions in the Cyanobacterial Circadian Clock:
681 Structure of KaiA Dimer in Complex with C-Terminal KaiC Peptides at 2.8 Angstrom
682 Resolution. *Biochemistry* **2015**, *54*, 4575–4578. <https://doi.org/10.2210/PDB5C5E/PDB>.

683 (58) Klaeger, S.; Heinzlmeir, S.; Wilhelm, M.; Polzer, H.; Vick, B.; Koenig, P. A.; Reinecke, M.;
684 Ruprecht, B.; Petzoldt, S.; Meng, C.; Zecha, J.; Reiter, K.; Qiao, H.; Helm, D.; Koch, H.; Schoof,
685 M.; Canevari, G.; Casale, E.; Depaolini, S. R.; Feuchtinger, A.; Wu, Z.; Schmidt, T.; Rueckert, L.;
686 Becker, W.; Huenges, J.; Garz, A. K.; Gohlke, B. O.; Zolg, D. P.; Kayser, G.; Vooder, T.;
687 Preissner, R.; Hahne, H.; Tonisson, N.; Kramer, K.; Gotze, K.; Bassermann, F.; Schlegl, J.;
688 Ehrlich, H. C.; Aiche, S.; Walch, A.; Greif, P. A.; Schneider, S.; Felder, E. R.; Ruland, J.; Medard,
689 G.; Jeremias, I.; Spiekermann, K.; Kuster, B. The Target Landscape of Clinical Kinase Drugs.
690 *Science (80-).* **2017**, *358*. <https://doi.org/10.2210/PDB5MAF/PDB>.

691 (59) Niefind, K.; Bischoff, N.; Golub, A. G.; Bdzhola, V. G.; Balandia, A. O.; Prykhod'ko, A. O.;
692 Yarmoluk, S. M. Structural Hypervariability of the Two Human Protein Kinase CK2 Catalytic
693 Subunit Paralogs Revealed by Complex Structures with a Flavonol- and a Thieno[2,3-
694 d]Pyrimidine-Based Inhibitor. *Pharmaceuticals* **2017**, *10*.
695 <https://doi.org/10.2210/PDB5M4F/PDB>.

696 (60) Brear, P.; De Fusco, C.; Hadje Georgiou, K.; Francis-Newton, N. J.; Stubbs, C. J.; Sore, H. F.;
697 Venkitaraman, A. R.; Abell, C.; Spring, D. R.; Hyvonen, M. Specific Inhibition of CK2 Alpha from
698 an Anchor Outside the Active Site. *Chem Sci* **2016**, *7*, 6839–6845.

699 https://doi.org/10.2210/PDB5CSP/PDB.

700 (61) Ohno, H.; Minamiguchi, D.; Nakamura, S.; Shu, K.; Okazaki, S.; Honda, M.; Misu, R.; Moriwaki, H.; Nakanishi, S.; Oishi, S.; Kinoshita, T.; Nakanishi, I.; Fujii, N. Structure-Activity Relationship Study of 4-(Thiazol-5-Yl)Benzoic Acid Derivatives as Potent Protein Kinase CK2 Inhibitors. *Bioorg. Med. Chem.* **2016**, *24*, 1136–1141. <https://doi.org/10.2210/PDB5B0X/PDB>.

704 (62) Boland, S.; Bourin, A.; Alen, J.; Geraets, J.; Schroeders, P.; Castermans, K.; Kindt, N.; Boumans, N.; Panitti, L.; Fransen, S.; Vanormelingen, J.; Stassen, J. M.; Leysen, D.; Defert, O. Design, Synthesis, and Biological Evaluation of Novel, Highly Active Soft ROCK Inhibitors. *J. Med. Chem.* **2015**, *58*, 4309–4324. <https://doi.org/10.2210/PDB4WOT/PDB>.

708 (63) Guerra, B.; Bischoff, N.; Bdzhola, V. G.; Yarmoluk, S. M.; Issinger, O. G.; Golub, A. G.; Niefind, K. A Note of Caution on the Role of Halogen Bonds for Protein Kinase/Inhibitor Recognition Suggested by High- And Low-Salt CK2 Alpha Complex Structures. *AcS Chem. Biol.* **2015**, *10*, 1654–1660. <https://doi.org/10.2210/PDB4UB7/PDB>.

712 (64) O'Reilly, M.; Cleasby, A.; Davies, T. G.; Hall, R. J.; Ludlow, R. F.; Murray, C. W.; Tisi, D.; Jhoti, H. Crystallographic Screening Using Ultra-Low-Molecular-Weight Ligands to Guide Drug Design. *Drug Discovery Today*. Elsevier Ltd May 2019, pp 1081–1086.

715 <https://doi.org/10.1016/j.drudis.2019.03.009>.

716 (65) Lee, T.; Hoofnagle, A. N.; Resing, K. A.; Ahn, N. G. Hydrogen Exchange Solvent Protection by an ATP Analogue Reveals Conformational Changes in ERK2 upon Activation. *J. Mol. Biol.* **2005**, *353* (3), 600–612. <https://doi.org/10.1016/j.jmb.2005.08.029>.

719 (66) Andersen, M. D.; Shaffer, J.; Jennings, P. A.; Adams, J. A. Structural Characterization of Protein Kinase A as a Function of Nucleotide Binding. Hydrogen-Deuterium Exchange Studies Using Matrix-Assisted Laser Desorption Ionization-Time of Flight Mass Spectrometry Detection. *J. Biol. Chem.* **2001**, *276* (17), 14204–14211. <https://doi.org/10.1074/jbc.M011543200>.

723 (67) Kleckner, I. R.; Foster, M. P. An Introduction to NMR-Based Approaches for Measuring Protein Dynamics. *Biochimica et Biophysica Acta - Proteins and Proteomics*. NIH Public Access August 2011, pp 942–968. <https://doi.org/10.1016/j.bbapap.2010.10.012>.

726 (68) Viegas, A.; Manso, J.; Nobrega, F. L.; Cabrita, E. J. Saturation-Transfer Difference (STD) NMR: A Simple and Fast Method for Ligand Screening and Characterization of Protein Binding. *J. Chem. Educ.* **2011**, *88* (7), 990–994. <https://doi.org/10.1021/ed101169t>.

729 (69) Lindenblatt, D.; Nickelsen, A.; Applegate, V.; Jose, J.; Niefind, K. Structural and Mechanistic

730 Basis of the Inhibitory Potency of Selected 2-Aminothiazole Compounds on Protein Kinase
731 CK2. *J. Med. Chem.* **2020**, acs.jmedchem.0c00587.
732 <https://doi.org/10.1021/acs.jmedchem.0c00587>.

733 (70) Lee, W.-K.; Son, S. H.; Jin, B.-S.; Na, J.-H.; Kim, S.-Y.; Kim, K.-H.; Kim, E. E.; Yu, Y. G.; Lee, H. H.
734 Structural and Functional Insights into the Regulation Mechanism of CK2 by IP6 and the
735 Intrinsically Disordered Protein Nopp140. *Proc. Natl. Acad. Sci.* **2013**, *110* (48), 19360–19365.
736 <https://doi.org/10.1073/pnas.1304670110>.

737 (71) Vom, A.; Headey, S.; Wang, G.; Capuano, B.; Yuriev, E.; Scanlon, M. J.; Simpson, J. S. Detection
738 and Prevention of Aggregation-Based False Positives in STD-NMR-Based Fragment Screening.
739 *Aust. J. Chem.* **2013**, *66* (12), 1518–1524. <https://doi.org/10.1071/CH13286>.

740 (72) Feng, B. Y.; Shoichet, B. K. A Detergent-Based Assay for the Detection of Promiscuous
741 Inhibitors. *Nat. Protoc.* **2006**, *1* (2), 550–553. <https://doi.org/10.1038/nprot.2006.77>.

742 (73) Shoichet, B. K. Screening in a Spirit Haunted World. *Drug Discov. Today* **2006**, *11* (13–14),
743 607–615. <https://doi.org/10.1016/j.drudis.2006.05.014>.

744 (74) Coan, K. E. D.; Maltby, D. A.; Burlingame, A. L.; Shoichet, B. K. Promiscuous Aggregate-Based
745 Inhibitors Promote Enzyme Unfolding. *J. Med. Chem.* **2009**, *52* (7), 2067–2075.
746 <https://doi.org/10.1021/jm801605r>.

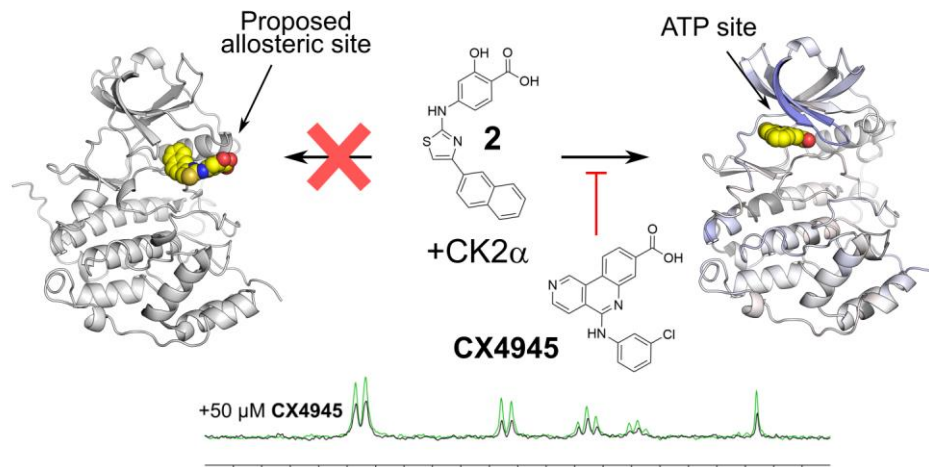
747 (75) McGovern, S. L.; Helfand, B. T.; Feng, B.; Shoichet, B. K. A Specific Mechanism of Nonspecific
748 Inhibition. *J. Med. Chem.* **2003**, *46* (20), 4265–4272. <https://doi.org/10.1021/jm030266r>.

749 (76) Walters, J.; Milam, S. L.; Clark, A. C. Chapter 1 Practical Approaches to Protein Folding and
750 Assembly. Spectroscopic Strategies in Thermodynamics and Kinetics. *Methods in Enzymology*.
751 NIH Public Access 2009, pp 1–39. [https://doi.org/10.1016/S0076-6879\(08\)04201-8](https://doi.org/10.1016/S0076-6879(08)04201-8).

752

753

754 Table of Content graphics



755